XLIII CILAMCE
21–25, November, 2022
FOZ DO IGUAÇU – PR – BRAZIL

Plastic Stress Concentration Factor K_F in Fatigue

Mengen Liu[a], Antonio Carlos de Oliveira Miranda[b1], Marco Antonio Meggiolaro[a], Jaime Tupiassú Pinho de Castro[a]

[a]*Mechanical Engineering Department, Pontifical Catholic University of Rio de Janeiro, Rua Marquês de São Vicente 225 – Gávea, Rio de Janeiro, RJ, 22451-900, Brazil*
meng9644@yahoo.com, meggi@puc-rio.br, jtcastro@puc-rio.br

[b]*Department of Civil and Environmental Engineering, University of Brasília, SG-12 Building, Darcy Ribeiro Campus, DF, 70.910-900, Brazil*
acmiranda@unb.br

Abstract. This study uses the stress gradient factors (SGFs) ahead of notch tips to determine the notch effects in fatigue, which are generally smaller than notch stress concentration factor due to the material tolerance to non-propagating short cracks. Even under elastic nominal stress levels, the notch vicinity may accumulate plastic strains when the maximum local stress exceeds the material yield strength. Considering the significant role of local plasticity in the propagation behavior of short cracks within the notch plastic zone and therefore in the notch sensitivity, a methodology is proposed to take into account the elastic-plastic stress and strain fields modeled by Neuber's rule and cyclic Ramberg-Osgood equation. 2D finite element analyses are conducted to compute the stress intensity factors (SIFs) of smooth and notched specimens, which in turn are used to calculate the SGFs and finally to obtain plastic fatigue notch factor predictions. To validate the methodology, experimental S-N data of centre-notched, U-notched and V-notched plate specimens made of different materials and tested at uniaxial load ratio R=-1, 0 and 0.1 are collected from the literature and compared with simulation results.

Keywords: Short cracks, stress gradient factor, notch-induced plasticity, fatigue plastic stress concentration factor, notch concentration..

1 Introduction

A wide variety of large structures, such as aircrafts, ships, metallic bridges must tolerate fatigue cracks during their service lives. These cracks can start and/or gradually grow due to the application of cyclic loads, which are inherent to their operational tasks. It is impossible to operate such structures without their presence, but their structural integrity must be ensured during their entire operational lives, providing the needed repair or replacement of eventually damaged structural components before these cracks can reach a critical size.

Almost all structural components have notches, the generic name for functional details associated with abrupt geometric transitions, which are required to assemble or to operate them, but locally concentrate or increase the nominal stress, σ_n, that would act at their location. Stress concentration effects are primordial importance for many failure mechanisms such as fatigue crack initiation, which cannot be property modeled without quantifying them. The simplest way to do so is by using stress concentration factor (SCF), $Kt = \sigma_{max}/\sigma_n$, to evaluate the maximum stress, σ_{max}, around the notch. However, although crack initiation at notch tips is always induced by the (Mises) combination of the several nominal stress components properly multiplied by their K_{ts}, the short crack propagation is also much affected by the stress gradients ahead of the critical notch tip. Therefore, the actual stress concentration effect for fatigue damage purposes is quantified by a fatigue stress concentration factor $K_f = S_L/S_L$'

[1] Corresponding author. Phone: +55-61-3107-0994; fax: +55-61- 3273-4644. E-mail: acmiranda@unb.br

≤ Kt, where S_L is the notched structural component fatigue limit and S_L' is its un-notched fatigue limit. K_f is related to notch sensitivity $q = (K_f - 1)/(K_t - 1)$.

Neuber and Peterson [1]–[3] were the pioneers to give solution about K_t and K_f, and other author has extended for different situations: the influence of grain size [4]–[10], in orthotropic materials [11]–[14], in composite materials [13], [15]–[19], for instance. An important aspect is consider the K_f as a short crack propagation [20]–[23], where a short crack propagates influenced by a stress gradient that, in certain cases, could stop when the level of stress decrease at crack tip. These approaches have more mechanics fundaments that others based on stress average on the notch, as methods used to compute K_f established on Theory of Critical Distance (TCD) [24]–[27], for instance. In fact, Antunes et al. [22] have suggested the application of the Stress Gradient Factor (SGF), an addition to Stress Intensity Factor (SIF), to TDC, given an interpretation that any critical distance should related to the SIF and fatigue stresses. In the perspective of K_f based on a short crack propagating through a stress gradient, in fact, notch sensibility should be named to "stress gradient sensitivity", to consider the similar behavior of notches, such as fretting, residual stress in welds and others that produce stress gradient.

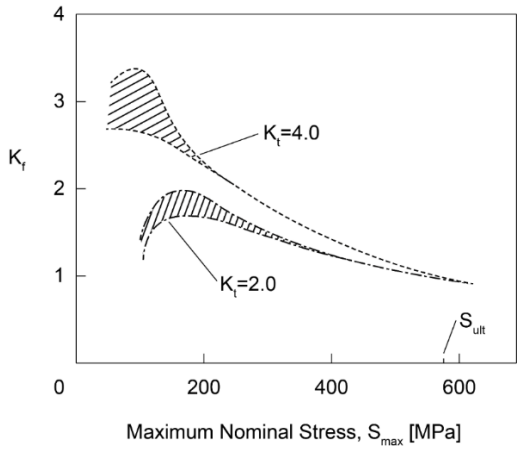

Fig. 1: The effect K_t and maximum nominal stress [28] to K_f.

Several experimental works evaluating stress-life behavior of notched components showed that K_f reduces at short cycles and high fatigue strengths, for example, the graph of a technical note presented in Figure 1 [28]. It is possible to clearly observe that K_f has a nonlinear behavior for all stress levels, with greater variation for sharp notches and it tends to the value of 1 when all the material is plasticated. Majzoobi and Daemi [29] investigated the effects of notch geometry on fatigue life for different materials divided into low-strength (LS) and high-strength (HS) steels. For LS steels, they observed that K_f depended on fatigue life and varied from a lower K_f for low-cycle fatigue tests to a higher K_f for high-cycle fatigue tests; on the other hand, for HS steels, no significant variation of K_f occurred. Authors of ASM Handbook [30] also affirmed that, for steels, K_f reduces at high stress levels, and such variation took place because of a reduction of the notch effect by plastic deformation. Juvinall and Marshek [31] mentioned the advice made by some references on neglecting the influence of notches at a short life of 103 cycles, but they found out it was valid only for relatively LS metals; and for relatively HS alloys of those same metals, the notch effect at short life is nearly equal to at a long life of 106 cycles. Nevertheless, they recommended the high-cycle elastic K_f be used in all cases, including the medium and low-cycle regimes. This practice is straightforward but may be overly conservative in low-cycle fatigue, where plastic yielding occurs around the notch tip.

The phenomenon of K_f variation with stress level in the finite life fatigue is well known and has several supporting experimental data in the literature. However, there is still a lack of studies and methods to predict notch sensitivity for medium-cycle and low-cycle regimes, where macroscopic plastic strains occur around notch tips and must be taken into account. Indeed, this issue analysis becomes more complicated and cannot be handled using only linear elastic solutions.

In a previous work, de Oliveira Miranda, et al. [32] proposed a stress gradient method with the SGF based on short crack concepts to predict the fatigue notch factor K_f for high-cycle fatigue regime, under linear elastic conditions. In this work, that original idea was extended to conduct the prediction of notch sensitivity in medium-

cycle and low-cycle regimes of S-N curve. To investigate the effects of material yielding around notch tips, Neuber's strain concentration rule and Ramberg-Osgood's cyclic strain-hardening model were employed. In addition, the Neuber rule was modified by replacing the stress with a stress intensity factor (SIF), and the strain with a strain-based intensity factor (SBIF), as proposed by El Haddad, et al [33]. In this case, since the K_f estimate is based on elastoplastic solutions, we denominated it as elastoplastic K_f in order to distinguish it from the traditional elastic K_f.

An additional contribution of this work is the correlation with the SGF with the TCD, proposed previously [22], offering a mechanical explanation for the critical distance, called here as a_{max}, and the equations for obtaining K_f. The work also offers a better understanding of some works that use the critical distance versus number of cycles relationship [26], [34]–[36].

2 Theorical Aspects

In inspection procedures of defects in a structure or a complex equipment, it is common to find some crack in notch roots, where ones propagates and others that does not. Therefore, it is possible to question why some cracks did not propagate significantly compared others. To explain why this behavior, it is necessary to use short crack tolerance concepts. Such concepts that there are small cracks called non-propagating cracks, which start, grow to a certain size, and then stop growing. To understand this process, it is necessary to use two fracture mechanics parameters: (1) $\Delta K_I(a)$, the Stress Intensity Factor (SIF), the crack driving force, and (2) the crack size dependent short Fatigue Crack Growth (FCG) threshold $\Delta K_{th,R}(a, a_R)$, a material property, were a_R is the so-called characteristic short crack size, namely $\mathbf{a_R = (1/\pi)(\Delta K_{th_R}/\eta \Delta S_{L_R})^2}$, ΔK_{thR} is the crack size independent FCG threshold and ΔS_{LR} is the fatigue limit range, both measured at a stress ratio $R = K_{min}/K_{max}$. Three possibilities can occur for the FCG behavior, if the crack is growing inside a stress field that has a steep gradient:

a) $\Delta K_I(a) > \Delta K_{th,R}(a, a_R)$ for all crack lengths, see Fig. 2(a). In this case, the crack propagates continually until the end of the load history, or else until the component fractures.
b) Initially $\Delta K_I(a) > \Delta K_{th,R}(a, a_R)$, so the short crack starts to grow increasing its length a across a decreasing stress field (whose gradient is quantified by its SGF), until its driving force $\Delta K_I(a)$ curve crosses its crack size dependent resistance curve $\Delta K_{th,R}(a, a_0)$, when the short crack reaches a size a_{st} in which $\Delta K_I(a_{st}) = \Delta K_{th,R}(a_{st}, a_0)$ and then stops. In this case, the crack becomes non-propagating (if the load $\{\Delta K(a_{st}), K_{max}(a_{st})\}$ is kept constant and if its resistance $\Delta K_{th,R}(a_{st}, a_0)$ remains time-independent), see Fig. 2(b).
c) Initially $\Delta K_I(a) > \Delta K_{th,R}(a, a_R)$ and the crack starts to grow until eventually the driving force $\Delta K_I(a)$ curve touches the crack resistance curve $\Delta K_{th,R}(a, a_0)$, but does not crosses it, see Fig. 2(c). This is the limiting condition to have a propagating crack. In the other hand, it defines as well the maximum size a_{max} a non-propagating short crack can reach under these loading and resistance conditions

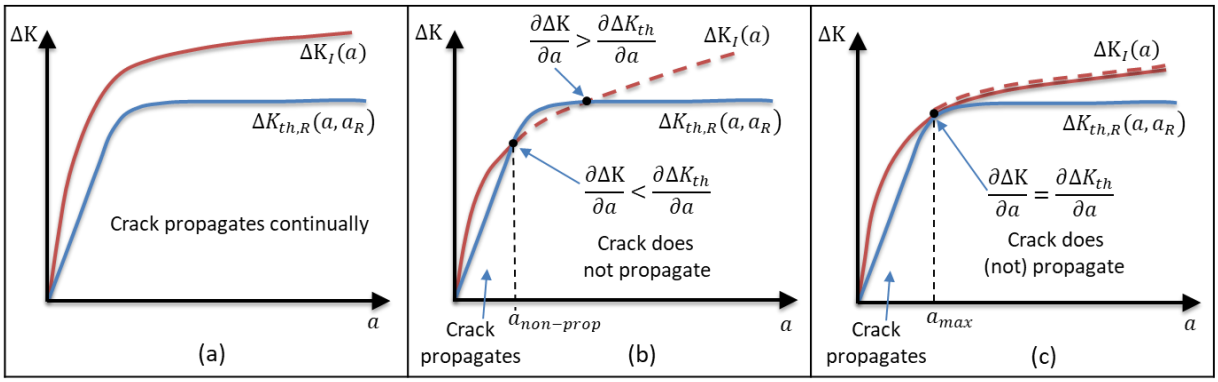

Fig. 2: (a) cracks grows continually, (b) crack grows and stops, and (c) crack growss and touches its crack-size dependent resistance curve, at the maximum non-propagating crack size a_{max}.

Therefore, in the fatigue analysis, the possibility of propagating and non-propagating cracks in critical places of the equipment must be verified. This concept of non-propagating cracks leads to the concept of defect tolerance fatigue analysis.

2.1 Fatigue Stress Concentration Factor

Following Castro et al. reasoning [37], a maximum short crack size a_{max}, Fig. 2(c), limits its growth/non-growth behavior. For any given loading/resistance pair, the tangency condition between the driving force and the FCG resistance curves of the growing short crack defines a_{max}:

$$\sigma_n\sqrt{\pi a_{max}}\cdot\eta\cdot f(a_{max}/w)\cdot K_{gr}(a_{max}/w) = \eta\cdot\Delta S_{L,R}\sqrt{\pi a_R}\cdot\left[1+(a_R/a_{max})^{\gamma/2}\right]^{-1/\gamma} \tag{1}$$

$$K_{gr}(a_{max}/w) = \underbrace{\frac{\Delta S_{L,R}}{\sigma_n}}_{const=K_f}\ \frac{1}{f(a_{max}/w)}\underbrace{\sqrt{\frac{a_R}{a}}\cdot\left[1+(a_R/a_{max})^{\gamma/2}\right]^{-1/\gamma}}_{h(a_R/a_{max},\gamma)} \tag{2}$$

where the term $const$ includes the fatigue (crack initiation) limit $\Delta S_{L,R}$, and the (constant) nominal stress σ_n, whereas $h(a_R/a,\gamma)$ is a function of a_R/a_{max} and γ. By deriving the last equation to take in account the tangency condition $\partial\Delta K/\partial a = \partial\Delta K_{th,R}/\partial a$:

$$\frac{\partial}{\partial a}\left[K_{gr}(a_{max}/w)\right] = const\ \frac{\partial}{\partial a}\left[\frac{h(a_R/a_{max},\gamma)}{f(a_{max}/w)}\right] \tag{3}$$

Isolating $const$ in last equation and substituting it back into equation (3), it is possible to obtain a_{max} by solving a simple non-linear equation (in compacted form):

$$K_{gr} - \frac{\partial K_{gr}}{\partial a}\left(\frac{h\cdot f}{\frac{\partial h}{\partial a}f - h\frac{\partial f}{\partial a}}\right) = 0 \tag{4}$$

Considering a function $k\left(\frac{a_R}{a_{max}},\gamma\right) = 2a_{max}\left[1+\left(\frac{a_R}{a_{max}}\right)^{\gamma/2}\right]$, the last equation becomes:

$$\frac{\frac{\partial(K_{gr}\cdot f)}{\partial a}k + K_{gr}\cdot f}{\frac{\partial f}{\partial a}k + f} = 0 \tag{5}$$

Equation (5) is more general than the similar equation presented by Miranda et al. [32], which did not incorporate the free surface factor η and required $f([a\to 0]/w)\to 1$. In that case, Eq. (5) can be written as:

$$\frac{\partial K_{gr}}{\partial a}k + K_{gr} = 0 \tag{6}$$

From equation (2), the elastic fatigue SCF K_f is obtained:

$$K_f = K_{gr}(a_{max}/w)\frac{\left[1+(a_R/a_{max})^{\gamma/2}\right]^{1/\gamma}}{\sqrt{a_R/a}} \tag{7}$$

3 Method

El Haddad, Smith, and Topper (ETS) originally proposed the concept of the Plastic Strain Gradient Factor (PSGF) in the short crack model in 1979 [38]. Indeed, it was implicit in their strain-based intensity factor (SBIF) range $\Delta K_{I\varepsilon}$ defined (for a Griffith plate) as

$$\Delta K_{I\varepsilon} = E\Delta e\sqrt{\pi(a+a_0)} \tag{8}$$

where Δe is the applied nominal strain range, E is the modulus of elasticity of material, a is the crack length, a_0 is the short crack characteristic size for pulsating loads. ETS also applied the SBIF for notched specimen, to

consider plastic strains around the notch tip. The nominal strain term Δe was replaced by the local strain in the vicinity of the crack (not the notch) tip $\Delta\varepsilon$. An estimative for $\Delta\varepsilon$ was proposed using Neuber's stress/strain concentration rule [39]. The strain-based intensity factor admits plasticity by replacing the conventional stress term by a strain term, to model short crack FCG in both elastic and plastic strain fields:

$$\Delta K_I = E\Delta\varepsilon_n\sqrt{\pi a}\cdot f(a/w)\cdot K_{gr\varepsilon}(a/w) \tag{9}$$

where $K_{gr\varepsilon}$ is the plastic strain SGF. The approach was used to predict elastic and inelastic short crack growth curves for notched specimens [38], [40], [33], [41].

Following the ideas proposed by ETS, a plastic stress SGF, $K_{gr\sigma}$, is defined here to find a plastic K_f in equation (7) by replacing K_{gr}, using plastic stress obtained from Neuber's rule. It is a popular way to correlate nominal stresses σ_n and strains ε_n with the elastoplastic (EP) stresses σ and strains ε they induce at notch roots. Neuber's equation states that the product between the stress and the strain concentration factors $K_\sigma = \sigma/\sigma_n$ and $K_\varepsilon = \varepsilon/\varepsilon_n$ is constant and equal to the square of the linear elastic (LE) or geometric stress concentration factor K_t, thus

$$K_t^2 = \frac{\sigma\cdot\varepsilon}{\sigma_n\cdot\varepsilon_n} \tag{10}$$

The same idea as the above equation can be used for the case of SFG:

$$\left[K_{gr}(a/w)\right]^2 = \frac{K_{I\sigma}\cdot K_{I\varepsilon}}{K_{I\sigma(reference)}\cdot K_{I\varepsilon(reference)}} = \frac{\sigma\sqrt{\pi a}\cdot f(a/w)\cdot E\varepsilon\sqrt{\pi a}\cdot f(a/w)}{\sigma_n\sqrt{\pi a}\cdot f_{ref}(a/w)\cdot E\varepsilon_n\sqrt{\pi a}\cdot f_{ref}(a/w)} \tag{11}$$

Whereas the size of the crack is too small, both geometric factors become $f(a/w)\rightarrow 1$ and $f_{ref}(a/w)\rightarrow 1$, given:

$$\left[K_{gr}(a/w)\right]^2 = \frac{\sigma\cdot\varepsilon}{\sigma_n\cdot\varepsilon_n} \tag{12}$$

Ramberg-Osgood is an empirical relation that can model the EP behavior of many materials. Its main limitation is do not recognize a purely LE behavior, and its main advantage is its mathematical simplicity. It describes EP monotonic and cyclic stress/strain curves considering strain-hardening by

$$\varepsilon = \frac{\sigma}{E} + \left(\frac{\sigma}{H}\right)^{\frac{1}{h}} \; and \; \Delta\varepsilon = \frac{\Delta\sigma}{E} + 2\left(\frac{\Delta\sigma}{2H_c}\right)^{\frac{1}{h_c}} \tag{13}$$

where E is the Young's modulus, H and h are the monotonic and H_c and h_c are the cyclic strain-hardening coefficients and exponents of the corresponding stress/strain curves of the material (H_c and h_c are measured on the stabilized cyclic stress/strain curve of the material, see e.g. [42]).

Local EP stresses and strains can be obtained from Eqs. (12) and (13), joining Neuber's rule and Ramberg-Osgood cyclic relation. To estimate the local (near to the crack tip) stress range gradient $\Delta\sigma(a/w)$ induced by the nominal stress range $\Delta\sigma_n$, by solving the resulting nonlinear equation for cyclic loads, following standard εN fatigue design procedures [42]:

$$\left[K_{gr}(a/w)\right]^2\left(\Delta\sigma_n^2 + \frac{2E\Delta\sigma_n^{\frac{(h_c+1)}{h_c}}}{(2H_c)^{\frac{1}{h_c}}}\right) = \left[\Delta\sigma(a/w)\right]^2 + \frac{2E\left[\Delta\sigma(a/w)\right]^{\frac{(h_c+1)}{h_c}}}{(2H_c)^{\frac{1}{h_c}}} \tag{14}$$

where H_c and h_c are the cyclic strain hardening coefficient and exponent measured on the stabilized cyclic stress/strain curve of the material.

Finally, the elastoplastic fatigue stress concentration, $K_{f(plastic)}$, is calculated by performing the following procedure:

1) Obtain the values of $\Delta K_{th,R}$ and $\Delta S_{L,R}$ of the unnotched geometry to calculate $a_R = \left(\frac{1}{\pi}\right)\left(\frac{\Delta K_{th,R}}{\Delta S_{L,R}}\right)^2$, as well as the cyclic properties of the stress-strain curve of the material.

2) Get linear stress distribution (discretized) ahead of the notch.
3) Compute $K_{gr}(a/w)$.
4) Compute the elastic value of $K_{f(elastic)}$, first with equation (6) and then with equation (7), and assigns the value $K_{f(current)}$=$K_{f(elastic)}$.
5) Get a stress value from a SN curve, ΔS, of the unnotched geometry and compute a nominal stress $\Delta\sigma_n = \Delta S/K_{f(current)}$.
6) Get the linear stress distribution (discretized), σ_i, ahead of the notch using $\Delta\sigma_n$ from previous step.
7) Compute a Neuber stress distribution, σ_{iN} for each σ_i.
8) Obtain $K_{gr(plastic)}(a/w)$ with the σ_{iN} stress distribution and using the procedure of step (3).
9) Compute the $K_{f(plastic)}$ with similar procedure of step (4).
10) Check a convergency test. If $K_{f(plastic)}$ is close to $K_{f(current)}$, with a tolerance (0.01, for example), $K_{f(plastic)}$ is the final value, and the procedure ends. Otherwise, $K_{f(current)} = K_{f(plastic)}$ and procedure should be returned to the step (5).

4 Validation

This section summarizes the procedures conducted to validate the proposed methodology. Experimental data of plain specimens S-N tests were fitted by a straight line in bi-logarithmic plot, where the knee point N_L was set on a typical number of cycles associated with fatigue limit measurement. In this work, it has been considered N_L=2x10^6 cycles for steels and N_L=5x10^8 cycles for aluminum alloys. From the obtained curve, 10 log-uniformly distributed stress range levels ΔS_i were chosen to be applied as the nominal stress range $\Delta\sigma_n$ in subsequent numerical simulations. For each stress range level, both elastic K_f and plastic K_f were computed, and the fatigue strengths of the notched specimens could be calculated. Subsequently, these values were fitted by straight lines in the bi-logarithmic plot to illustrate the S-N curves of notched specimens predicted separately by ESGF and PSGF. Finally, the experimental data of notched specimens S-N tests were also plotted to compare with the predictions.

4.1 Specimens and materials

The experimental data of S-N tests on notched and plain specimens reported by [26], [43], [44] were considered for the investigation. Figure 3 schematizes the geometries of notched specimens: a) strip with a central circular hole of radius ρ; b) strip with a single U-shaped notch of depth b and radius ρ; c) strip with a single 60º V-shaped notch of depth b and radius ρ. All the geometries have a finite weight and are under axial loadings. Table 1 shows mechanical properties of the materials of specimens tested under tension-compression (R=-1), pulsating tension (R=0) and tension-tension (R=0.1) loadings. The ETS short crack characteristic lengths a_0. The values of H_c and h_c for 2024-T351 and SAE1020 were reported in [35], and those for SAE1045 were determined using the least squares method to fit experimental cyclic stress-strain curves [20] by the cyclic Ramberg-Osgood relationship. It is worth emphasizing that the value of strain hardening parameters may vary significantly depending on the curve-fitting technics used to obtain them.

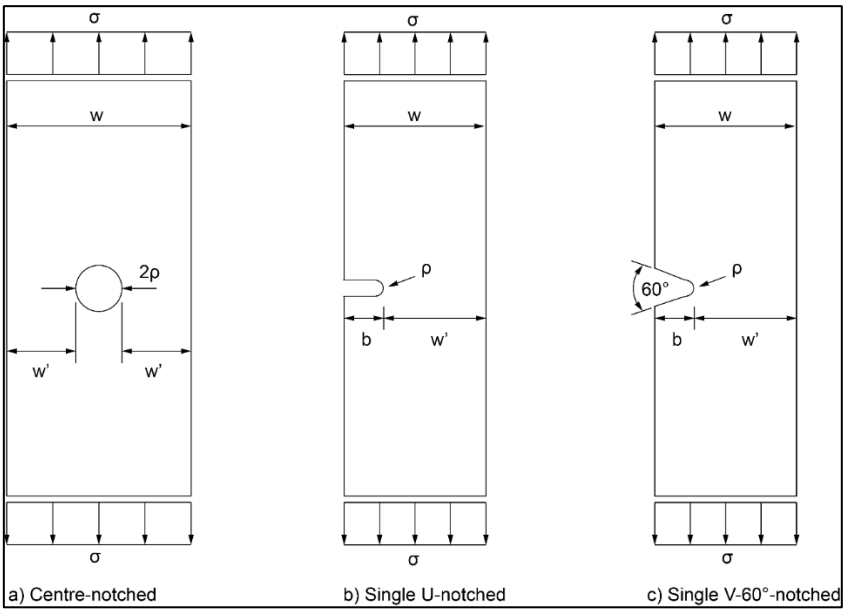

Fig. 3: Specimen geometries.

Table 1: Materials properties.

Material	R	E (GPa)	S_y (MPa)	H_c (MPa)	h_c (MPa)	ΔS_L (MPa)	ΔK_{th} (MPa$\sqrt{m}$)	a_0 (mm)
2024-T351 Al	-1	72.4	356.5	957	0.166	248	3.52	0.051
SAE1045	-1	206	390	1133.0	0.1696	604	9	0.056
	0	206	390	1133.0	0.1696	448	6.9	0.060
SAE1045 (T1200)	-1	206	645	1376.0	0.1661	760	7.7	0.026
SAE1045 (T900)	-1	206	1054	1417.2	0.1055	1134	6.98	0.010
SAE1045 (T600)	-1	206	1617	5098.8	0.2292	1200	7.5	0.010
SAE1020	-1	197.4	606.2	890.7	0.1635	412.6	16.2	0.390
	0.1	197.4	606.2	890.7	0.1635	327.6	11.8	0.328

*All SAE1045 steels have the same chemical composition but differ in their microstructures modified by the heat treatment: as-received ferrite-perlite and quenched-tempered martensite (oil quenching and tempering at 1200, 900 and 600°F, respectively, which are equivalent to 649, 482 and 315°C) [20].

Table 2 shows the geometry dimensions of the analyzed specimens in millimeters, their elastic stress concentration factors Kt calculated by finite element method based on the gross area, and predicted values of K_f and maximum tolerable crack length in millimeters under elastic conditions. The K_f obtained by ESGF and the associated a_{max} are both elastic parameters, thus do not depend on the applied stress level.

Table 2: Notched specimens geometries.

Material	R	Geometry	w	b	ρ	K_t	$K_{f,el}$	$a_{max,el}$
2024-T351 Al	-1	Centre-notched	44.6	0.12	0.12	3.02	2.175	0.053
			44.6	0.25	0.25	3.06	2.594	0.045
			44.6	0.5	0.5	3.06	2.849	0.035
			44.6	1.5	1.5	3.06	3.005	0.024
SAE1045	-1	Centre-notched	44.45	0.12	0.12	3.01	2.111	0.059
			44.45	0.25	0.25	3.04	2.537	0.051
			44.45	0.5	0.5	3.05	2.815	0.040
			44.45	1.5	1.5	3.05	2.989	0.027
SAE1045	0	Centre-notched	44.45	0.12	0.12	3.01	2.073	0.064
			44.45	0.25	0.25	3.04	2.502	0.055

			44.45	0.5	0.5	3.05	2.795	0.044
			44.45	1.5	1.5	3.05	2.984	0.029
SAE1045 T1200	-1	Centre-notched	44.45	0.12	0.12	3.01	2.539	0.023
			44.45	0.5	0.5	3.05	2.962	0.014
			44.45	1.5	1.5	3.05	3.025	0.009
SAE1045 T900	-1	Centre-notched	44.45	0.12	0.12	3.01	2.863	0.006
			44.45	0.5	0.5	3.05	3.024	0.004
			44.45	1.5	1.5	3.05	3.038	0.002
SAE1045 T600	-1	Centre-notched	44.45	0.12	0.12	3.01	2.857	0.006
			44.45	0.5	0.5	3.05	3.023	0.004
			44.45	1.5	1.5	3.05	3.038	0.003
SAE1020	-1	Centre-notched	25	4	4	3.45	3.208	0.269
			25	1.75	1.75	3.10	2.579	0.352
		U-notched	25	5	1.5	6.16	5.120	0.053
		V-notched	25	4	0.12	16.56	5.122	0.045
SAE1020	0.1	Centre-notched	25	4	4	3.45	3.255	0.035
			25	1.75	1.75	3.10	2.664	0.024
		U-notched	25	5	1.5	6.16	5.289	0.059
		V-notched	25	4	0.12	16.56	5.556	0.051

There were some limitations in collecting experimental data from the literature to validate the methodology, as described below:

- The present work aims to evaluate the notch stress gradient effect for specimens tested under axial loadings. However, stress-life tests with this loading type, conducted in servo-hydraulic testing machines, are more expansive than those in rotary bending testing machines. This fact turns running extensive axial S-N testing less viable.
- The fatigue propagation threshold ΔK_{th} is a fundamental property to calculate the ETS short crack characteristic length, and so are H_c and h_c to describe the cyclic strain-hardening behavior of materials by Ramberg-Osgood model. However, these material properties are frequently not reported by authors in experimental research works. On the other hand, estimating these properties may lead to erroneous predictions since their values reported in the literature show large scatters [45].

4.2 Results and discussions

Figs. 4-11 show the predicted S-N curves for notched specimens of SAE1045 steels (the as-received and the heat-treated ones) and their experimental data under stress ratio R=-1. It should be noted that the experimental data of plain specimens are scattered because S-N tests are usually affected by various factors, e.g., sample surface, alignment of testing machine and specimens, environmental conditions, etc.

In the fatigue strength region, i.e., where the number of cycles is larger than the knee point N_L, the fatigue limit of notched specimens must be obtained considering the elastic K_f. By definition, the fatigue strength against crack initiation is the stress below which the material does not accumulate fatigue damage, i.e., it must be free from macroscale cyclic plastic strains.

For each material and notched geometry, the S-N curve predicted using elastic K_f is always parallel to the curve of plain specimens. On the other hand, numerical results show that plastic K_f should diminish with increasing stress levels that induce larger amplitudes of plasticity around the notch root. The different slope of the curve predicted using plastic K_f illustrates its variation according to changes in the stress level.

In fact, the variation in plastic K_f is related to the stress gradient ahead of the notch root when small-scale plastic strains are present around there. As the strength of the material within the plastic zone increases by strain-hardening, the maximum local stress also increases, raising the local stress gradient factors, which in turn affects

the behavior of short cracks propagating there. Thus, the evaluation of cyclic Ramberg-Osgood parameters plays a fundamental role in the analysis of plastic K_f, as will be discussed later.

It is worth mentioning the fatigue life of SAE1045 steel specimens tested at R=-1 is plotted against the nominal elastoplastic parameter, $(\Delta S \Delta \varepsilon E)^{1/2}$, as presented by the original authors. This parameter is equivalent to nominal stress for notched specimens since all the applied stress levels were elastic.

Fig. 4 shows the results obtained for specimens of as-received SAE1045 steel tested at R=-1, where the hole radius is 0.12, 0.25, 0.5 and 1.5mm, respectively. Within this notch size range, the notch sensitivity decreases as the notch root radius decreases. In Fig. 4(a), the S-N data measured in notched specimens are scattered, and most of them represent experimental K_f between the predicted values of elastic and plastic K_f. In Fig. 4(b) and (c), the experimental data of notched specimens are better described by the plastic K_f predicted curves, demonstrating that the fatigue notch factor indeed depends on the stress-strain conditions in the finite life region.

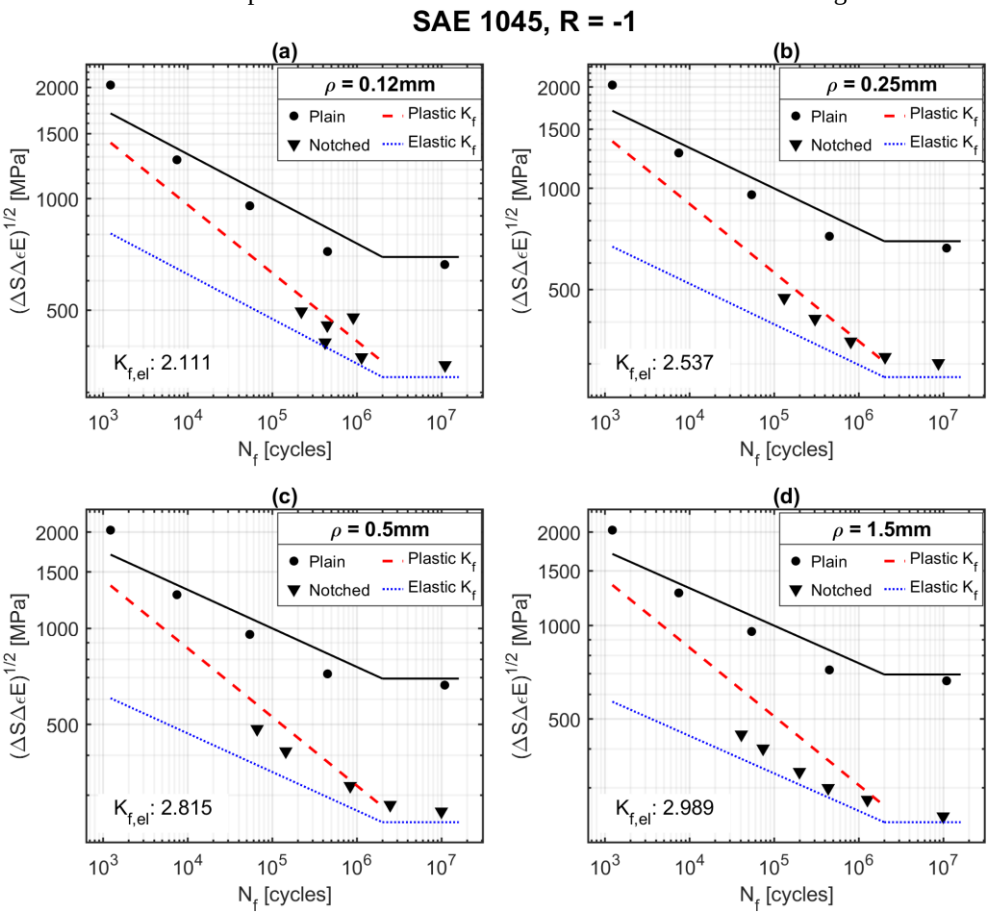

Fig. 4: S-N curve predictions for notched specimens of SAE1045 steel at R=-1

Figs. 5-6 show results obtained for SAE1045 T1200 and T900 steels, respectively, in notched components with the radius of the central hole equal to 0.12, 0.5 and 1.5mm. The predictions well described all the experimental data: K_f values lean toward the elastic prediction at lower stress levels and the plastic one at higher stress levels, where the plastic strains cannot be ignored.

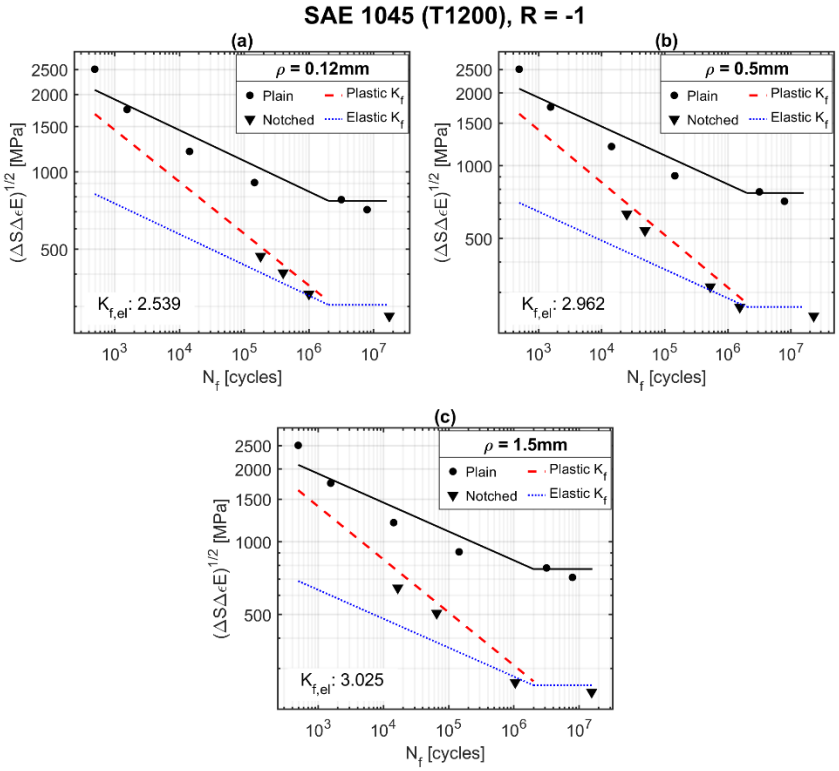

Fig. 5: S-N curve predictions for notched specimens of SAE1045 (T1200) steel at R=-1.

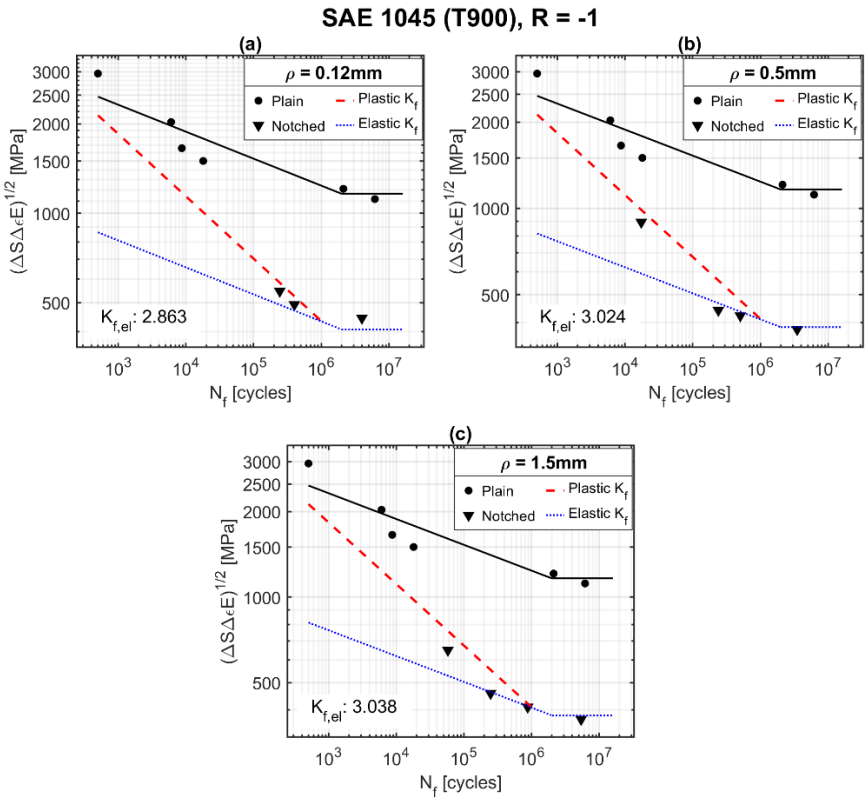

Fig. 6: S-N curve predictions for notched specimens of SAE1045 (T900) steel at R=-1.

Table 1 shows that the ETS short crack lengths of SAE1045 T900 and T600 steels are very similar, despite their different fatigue limits and propagation thresholds. Consequently, the numerical model also predicted very similar elastic K_f values for each geometry of two steels, as shown in Figs. 6-7. However, under elastoplastic conditions, their plastic K_f variations in function of stress level show different behaviors according to the strain-

hardening parameters of the materials. As SAE1045 T600 steel substantially strengthens by plastic deformation due to the high values of h_c and H_c (see Table 1), the amplitude of local plasticity induced by elastoplastic stress should be smaller than it would be in the other SAE1045 steels that have lower h_c and H_c. This explains why the difference between elastic and plastic predictions of K_f for T600 is softer compared to T900.

For all analyzed notch sizes for SAE1045 T900 and T600, the predicted a_{max} lengths under elastic conditions are extremely tiny, within the range of 1-10μm. In other words, they can only tolerate very small defects that would stop propagating by fatigue. Consequently, their elastic K_f values tend to be the respective theoretical notch factors, K_t.

Nonetheless, discrepancies between the experimental data and the numerical estimates of K_f values for SAE1045 T600 should be noted in Fig. 7. The elastic K_f prediction appears to be conservative for all three notch sizes. In addition, the plastic K_f predictions could not satisfactorily describe the experimental data in the finite life regimes of Fig. 7(a) and (b). The problem is possibly related to Ramberg-Osgood parameters used to model the strain-hardening behavior. Proper assessment of the strain field around crack tip within the notch-induced plastic zone is essential to quantify its effect through strain-based intensity factors and to estimate fatigue notch factors through PSGFs.

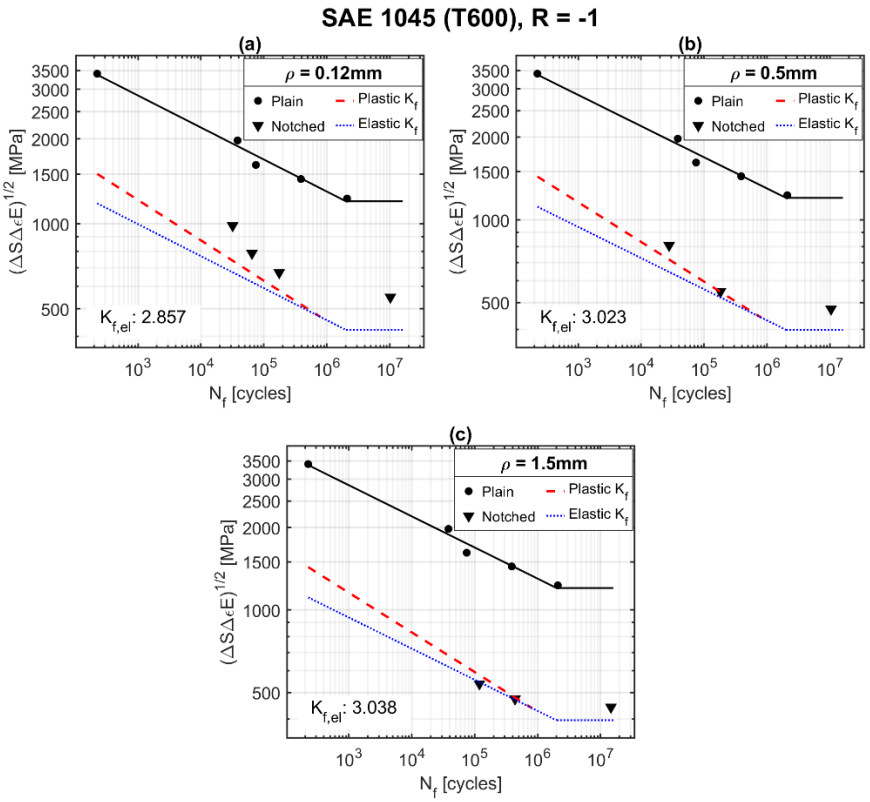

Fig. 7: S-N curve predictions for notched specimens of SAE1045 (T600) steel at R=-1.

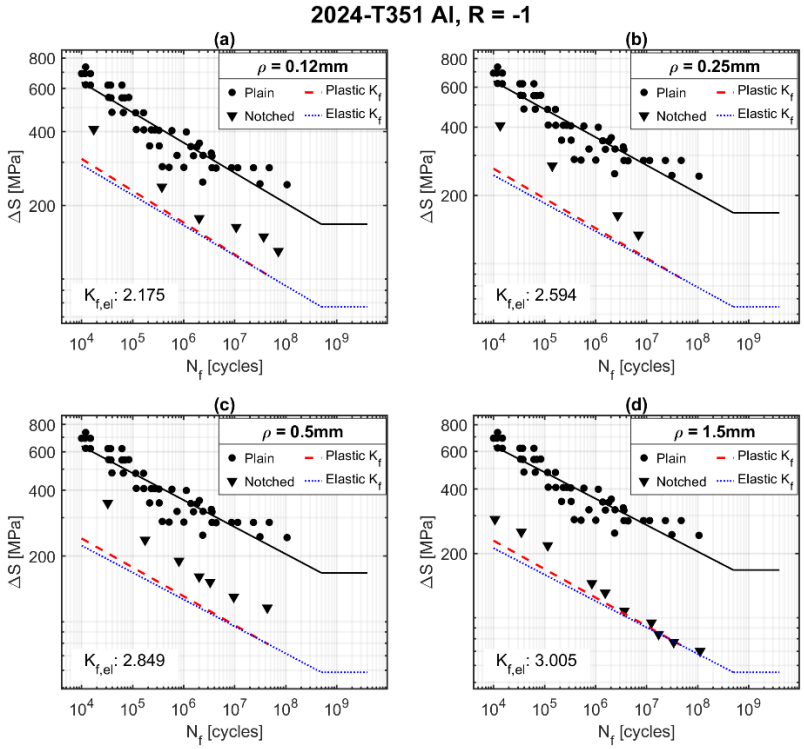

Fig. 8: S-N curve predictions for notched specimens of 2024 T351 Al, R=-1.

Fig. 8 shows predictions for notched specimens of 2024 T351 Al alloy with central hole radii equal to 0.12, 0.25, 0.5 and 1.5mm. Some S-N tests on plain specimens were terminated before the fatigue life of $5x10^8$ cycles was reached. Thus, the fatigue limit of the material was not properly determined, which directly affects the calculation of ETS length and the subsequent K_f prediction.

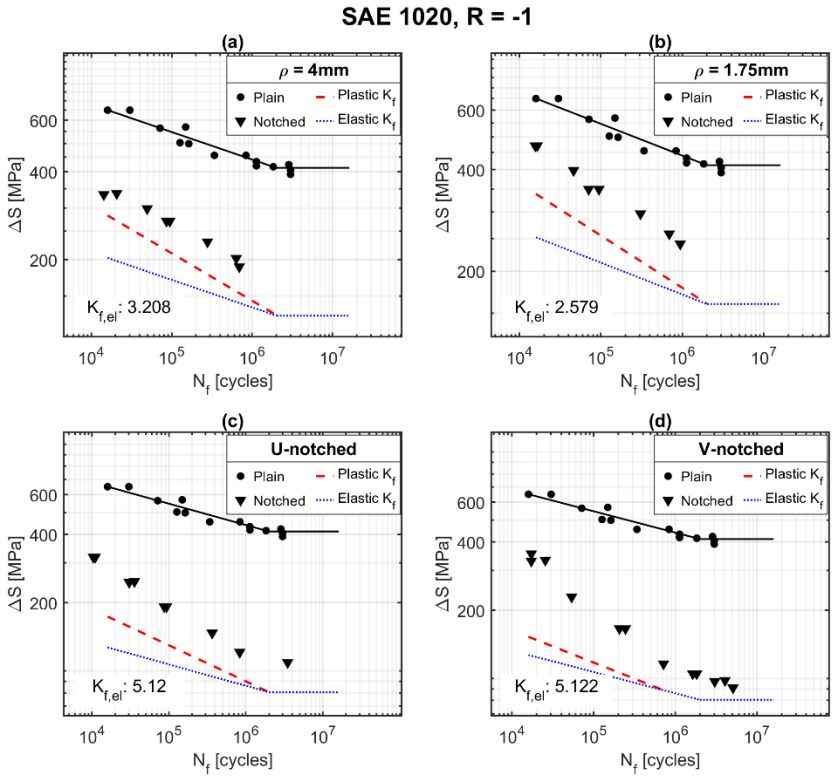

Fig. 9: S-N curve predictions for notched specimens of SAE1020, R=-1.

Fig. 9 shows the comparisons obtained for SAE1020 steel at R=-1. The predictions of K_f for the material and stress ratio are conservative for all four notch geometries. On the other hand, it can be observed that the

experimental K_f value varies with the stress level, and the slope of the predicted plastic K_f curve can describe this trend well, although conservative in general.

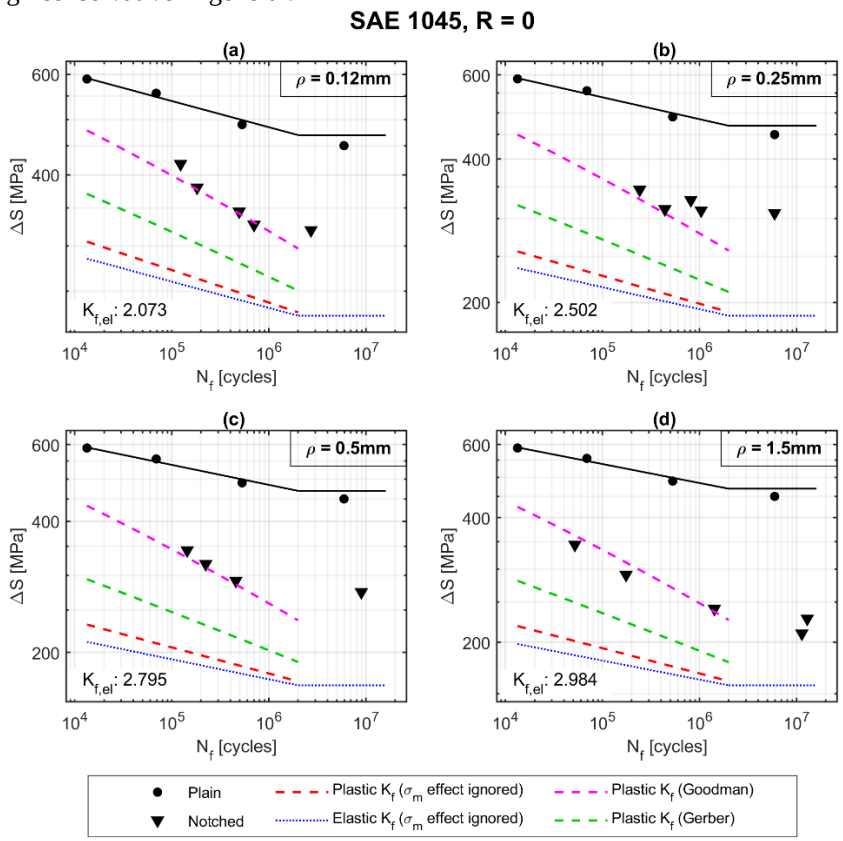

Fig. 10: S-N curve predictions for notched specimens of SAE1045, R=0.

Figs. 10-11 show the results obtained for as-received SAE1045 and SAE1020 steels at R≥0. The fatigue properties used to calculate ETS lengths were measured at the respective stress ratios with tensile mean stresses. Unlike the predictions for as-received SAE1045 steel under zero mean stress (which are in great agreement with the corresponding experimental data), those under non-zero mean stress performed conservatively for both finite and infinite life regimes with no correction of mean stress effects. Figs show the two classic corrections of mean stress: Gerber and Goodman corrections. For SAE1045 and R=0, in Fig 10, Goodman approach gives better prediction. However, for SAE1020 and R=0.1, Fig. 11, Gerber approach presents better prediction. These two approaches are classic well know methods of literature and the results show why they correct the mean stress better for some material, in opposite of each one.

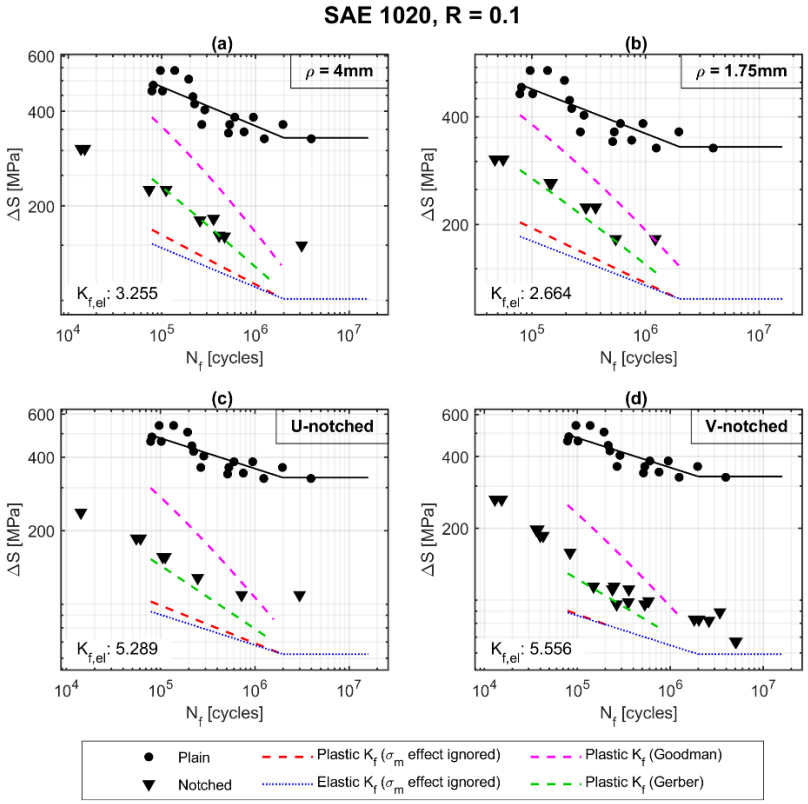

Fig. 11: S-N curve predictions for notched specimens of SAE1020, R=0.1.

5 Conclusion

This work presented the possibility of a plastic fatigue stress concentration factor, being used to estimate notched SN fatigue curves from unnotched component curves. The calculation is based on fracture mechanics based on deformation for short cracks that propagate in local plastic envelopes and in stress gradients. Using the stress gradient factor K_{gr}, a FIT, it is possible to calculate an elastic K_f in a single equation that relates to an a_{max}, the maximum size that the short crack can propagate until it stops. The calculation of plastic K_f is carry out by an iterative process using Neuber's rule and the cyclic constitutive equation of the material. The entire process is based on the short crack behavior from the fracture mechanics. The results presented compared with data from the literature show a positive correlation.

Another result obtained in this work is how the proposed development relates to the methods of the Theory of Critical Distance (TCD). The TCD basically uses three methods for calculating linear K_f, with different values of critical distances. This work shows that the critical distances are equivalent to a_{max}, as well as the distance and area methods are obtained from the K_f equation of the gradient method using Kgr. The work also shows that the relationship between the critical distance (a_{max}) and the number of cycles is unrealistic, since a_{max} naturally obtained from the behavior of short cracks.

The use of the design philosophy based on defect tolerance, as shown in this work, can be extended in other directions. As it was applied to notches, it can be applied in situations of unnotched components, such as butt welds and contact between bodies, for example. In this way the term notch sensitivity could be redefined to stress gradient sensitivity. Another natural extension is to apply the ideas for the εN method using strain-based fracture mechanics. Therefore, this paper opens other avenues to be explored in the future

References

[1] H. Neuber, *Kerbspannungslehre: Theorie der Spannungskonzentration Genaue Berechnung der Festigkeit*. Springer-Verlag, 1946.

[2] R. E. Peterson, *Stress Concentration Design Factors*. J. Wiley & Sons, 1953.

[3] R. E. Peterson, "Notch sensitivity," *Met. fatigue*, pp. 293–306, 1959.

[4] M. D. Chapetti, N. Katsura, T. Tagawa, and T. Miyata, "Static strengthening and fatigue blunt-notch sensitivity in low-carbon steels," *Int. J. Fatigue*, vol. 23, no. 3, pp. 207–214, 2001.

[5] E. M. Schulson and J. A. Roy, "The notch-sensitivity of ordered Zr3Al," *J. Nucl. Mater.*, vol. 71, no. 1, pp. 124–133, 1977.

[6] S. M. J. Razavi, B. Van Hooreweder, and F. Berto, "Effect of build thickness and geometry on quasi-static and fatigue behavior of Ti-6Al-4V produced by Electron Beam Melting," *Addit. Manuf.*, vol. 36, p. 101426, 2020.

[7] P. Lorenzino and A. Navarro, "Influence of the ratio between specimen thickness and grain size on the fatigue and tensile properties of plain and notched aluminium plate specimens," *Int. J. Fatigue*, p. 107149, 2022.

[8] M. D. Chapetti, H. Miyata, T. Tagawa, T. Miyata, and M. Fujioka, "Fatigue strength of ultra-fine grained steels," *Mater. Sci. Eng. A*, vol. 381, no. 1, pp. 331–336, 2004.

[9] P. Lorenzino and A. Navarro, "Grain size effects on notch sensitivity," *Int. J. Fatigue*, vol. 70, pp. 205–215, 2015.

[10] S. V Sajadifar, T. Wegener, G. G. Yapici, and T. Niendorf, "Effect of grain size on the very high cycle fatigue behavior and notch sensitivity of titanium," *Theor. Appl. Fract. Mech.*, vol. 104, p. 102362, 2019.

[11] M. Kawai and Y. Arai, "Off-axis notched strength of fiber–metal laminates and a formula for predicting anisotropic size effect," *Compos. Part A Appl. Sci. Manuf.*, vol. 40, no. 12, pp. 1900–1910, 2009.

[12] W. H. Alhazmi *et al.*, "Notch Tensile Strength of Carbon Fiber/Epoxy Composite Plate with a Center Hole under Static and Cyclic Loading," *Procedia Struct. Integr.*, vol. 17, pp. 292–299, 2019.

[13] M. Zappalorto, "Static notch sensitivity in orthotropic materials and composites," *Eur. J. Mech. - A/Solids*, vol. 85, p. 104094, 2021.

[14] M. Zappalorto and M. Ricotta, "Understanding the effect of notches in orthotropic solids subjected to static loads," *Theor. Appl. Fract. Mech.*, vol. 116, p. 103110, 2021.

[15] S. M. Bishop, "Effect of moisture on the notch sensitivity of carbon fibre composites," *Composites*, vol. 14, no. 3, pp. 201–205, 1983.

[16] M.-Y. He, B. Wu, and Z. Suo, "Notch-sensitivity and shear bands in brittle matrix composites," *Acta Metall. Mater.*, vol. 42, no. 9, pp. 3065–3070, 1994.

[17] S. T. Mileiko, "Fracture-toughness/notch-sensitivity correlation for metal- and ceramic-based fibrous composites," *Compos. Part B Eng.*, vol. 116, pp. 1–6, 2017.

[18] T. Mamiya, H. Kakisawa, W. H. Liu, S. J. Zhu, and Y. Kagawa, "Tensile damage evolution and notch sensitivity of Al2O3 fiber-ZrO2 matrix minicomposite-reinforced Al2O3 matrix composites," *Mater. Sci. Eng. A*, vol. 325, no. 1, pp. 405–413, 2002.

[19] M. R. Wisnom, "8.6 Notch Sensitivity of Composites," P. W. R. Beaumont and C. H. B. T.-C. C. M. I. I. Zweben, Eds. Oxford: Elsevier, 2018, pp. 98–117.

[20] E. M. Fontes do Rêgo, M. A. Antunes, and A. C. de Oliveira Miranda, "A methodology for fretting fatigue life estimation using strain-based fracture mechanics," *Eng. Fract. Mech.*, vol. 194, pp. 24–41, Mar. 2018.

[21] A. C. de Oliveira Miranda, M. A. Antunes, M. V. Guamán Alarcón, M. A. Meggiolaro, and J. T. Pinho de Castro, "Use of the stress gradient factor to estimate fatigue stress concentration factors K," *Eng. Fract. Mech.*, vol. 206, pp. 250–266, Feb. 2019.

[22] M. A. Antunes, C. R. M. da Silva, E. M. F. do Rêgo, and A. C. de Oliveira Miranda, "Stress intensity factor solutions for fretting fatigue using stress gradient factor," *Eng. Fract. Mech.*, vol. 186, pp. 331–346, Dec. 2017.

[23] M. A. Meggiolaro, A. C. d. O. Miranda, and J. T. P. de Castro, "Short crack threshold estimates to predict notch sensitivity factors in fatigue," *Int. J. Fatigue*, vol. 29, no. 9–11, 2007.

[24] D. Taylor, *The Theory of Critical Distances: A New Perspective in Fracture Mechanics*. Elsevier Science, 2010.

[25] D. Taylor, "The theory of critical distances," *Eng. Fract. Mech.*, vol. 75, no. 7, pp. 1696–1705, 2008.

[26] L. SUSMEL and D. TAYLOR, "A novel formulation of the theory of critical distances to estimate lifetime of notched components in the medium-cycle fatigue regime," *Fatigue Fract. Eng. Mater. Struct.*, vol. 30, no. 7, pp. 567–581, Jul. 2007.

[27] D. Taylor, *The theory of critical distances - A new perspective in fracture mechanics*, 1st ed. Elsevier, 2007.

[28] W. Llly, "Fatigue Tests in Notched and Unnotched Sheet Speciments of 2020-T3 Aluminium Alloys and of SAE 4130 Steel with Special Consideration of he Life from 2 to 10,000 Cycles," Washington, 1956.

[29] G. H. Majzoobi and N. Daemi, "The effects of notch geometry on fatigue life using notch sensitivity factor," *Trans. Indian Inst. Met.*, vol. 63, no. 2, pp. 547–552, 2010.

[30] A. S. M. H. Committee, "Properties and Selection: Irons, Steels, and High-Performance Alloys." ASM International, 01-Jan-1990.

[31] R. C. Juvinall and K. M. Marshek, *Fundamentals of Machine Component Design*. Wiley, 2020.

[32] A. C. de Oliveira Miranda, M. A. Antunes, M. V. Guamán Alarcón, M. A. Meggiolaro, and J. T. Pinho de Castro, "Use of the stress gradient factor to estimate fatigue stress concentration factors Kf," *Eng. Fract. Mech.*, vol. 206, pp. 250–266, 2019.

[33] M. H. El Haddad, K. N. Smith, and T. H. Topper, "A Strain Based Intensity Factor Solution for Short Fatigue Cracks Initiating from Notches," in *Fracture Mechanics: Proceedings of the Eleventh National Symposium on Fracture Mechanics: Part I*, C. W. Smith, Ed. West Conshohocken, PA: ASTM International, 1979, pp. 274–289.

[34] J. A. Araújo, F. C. Castro, I. M. Matos, and R. A. Cardoso, "Life prediction in multiaxial high cycle fretting fatigue," *Int. J. Fatigue*, vol. 134, p. 105504, 2020.

[35] Y.-L. Wu, S.-P. Zhu, J.-C. He, D. Liao, and Q. Wang, "Assessment of notch fatigue and size effect using stress field intensity approach," *Int. J. Fatigue*, vol. 149, p. 106279, 2021.

[36] S.-P. Zhu, J.-C. He, D. Liao, Q. Wang, and Y. Liu, "The effect of notch size on critical distance and fatigue life predictions," *Mater. Des.*, vol. 196, p. 109095, 2020.

[37] J. T. P. D. Castro, M. A. Meggiolaro, A. C. D. O. Miranda, H. Wu, A. Imad, and N. Benseddiq, "Prediction of fatigue crack initiation lives at elongated notch roots using short crack concepts," *Int. J. Fatigue*, vol. 42, 2012.

[38] M. H. El Haddad, K. N. Smith, and T. H. Topper, "Fatigue Crack Propagation of Short Cracks," *J. Eng. Mater.*

Technol., vol. 101, no. 1, pp. 42–46, Jan. 1979.
[39] H. Neuber, "Theory of Stress Concentration for Shear-Strained Prismatical Bodies With Arbitrary Nonlinear Stress-Strain Law," *J. Appl. Mech.*, vol. 28, no. 4, pp. 544–550, Dec. 1961.
[40] M. H. El Haddad, T. H. Topper, and K. N. Smith, "Prediction of non propagating cracks," *Eng. Fract. Mech.*, vol. 11, no. 3, pp. 573–584, 1979.
[41] M. H. El Haddad, T. H. Topper, and T. N. Topper, "Fatigue Life Predictions of Smooth and Notched Specimens Based on Fracture Mechanics," *J. Eng. Mater. Technol.*, vol. 103, no. 2, pp. 91–96, Apr. 1981.
[42] M. A. Castro, Jaime Tupiassu Pinho and Meggiolaro, "Fatigue design techniques: : Low-Cycle and Multiaxial Fatigue," *CreateSpace, Scotts Valley, CA, USA*, vol. 2. CreateSpace Independent Publishing Platform, 2016.
[43] D. L. Duquesnay, T. H. Topper, M. T. Yu, and A. M. Bertetto, "The Effect of Notch Radius on the Fatigue Notch Factor and the Propagation of Short Cracks," in *Mechanical Engineering Publications, The Behaviour of Short Fatigue Cracks*, 1986, pp. 323–335.
[44] M. T. Yu, D. L. DuQuesnay, and T. H. Topper, "Notch fatigue behaviour of SAE1045 steel," *Int. J. Fatigue*, vol. 10, no. 2, pp. 109–116, 1988.
[45] M. A. Meggiolaro and J. T. P. Castro, "Statistical evaluation of strain-life fatigue crack initiation predictions," *Int. J. Fatigue*, vol. 26, no. 5, pp. 463–476, 2004.